Preparation and Characterization of P_2O_5 Containing Canasite Glass-Ceramics as Potential Materials for Dental Restorations

Zahra Shamohammadi Ghahsareh, Sara Banijamali*, Alireza Aghaei

* banijamali@merc.ac.ir, banijamalis@yahoo.com

Ceramic Department, Materials and Energy Research Center (MERC), Alborz, Iran. (P. O. Box: 31787-316)

Abstract: Various analysis techniques were used to investigate the effects of P_2O_5 on the crystallization, mechanical features, and chemical resistance of canasite-based glass-ceramics. The results showed that canasite-type crystals were the primary crystalline phase in the examined glass-ceramics subjected to the two-step heat treatment, while fluorapatite was the secondary crystalline phase in some specimens. The microstructural observations by field emission electron microscope indicated that the randomly oriented interlocked blade-like canasite crystals decreased with an increase in the P_2O_5 content of the parent glasses. Among the examined glass-ceramics, the Base-P2 composition (containing 2 weight ratios of P_2O_5 in the glass) showed the most promising mechanical features (flexural strength of 176 MPa and fracture toughness of 2.9 $MPa.m^{1/2}$) and chemical resistance (solubility of 2568 $\mu g/cm^2$). This glass-ceramic could be further considered as a core material for dental restorations.

Keywords: Glass-ceramic, Dental restorations, Canasite, Mechanical properties, Chemical durability.

1. INTRODUCTION

Dental ceramics are divided into two groups of bioactive and bio-inert materials. Bioactive ceramics are used in periodontal healing, hypersensitivity treatment, bone regeneration, substitutes, and implant coatings; whereas bio-inert ceramics are mainly utilized as the biocompatible and inert dental restorations. Among restorative ceramics, glass-ceramic materials have drawn growingly attention due to their low thermal conductivity, high compressive strength, natural appearance, and appropriate abrasion resistance. Contrary of these priorities, dental applications of glass-ceramic materials have been restricted because of their low tensile strength, brittle nature, sensitivity to defects and flaws as well as their low fracture toughness [1-3]. These materials could be used to reconstruct teeth as onlays, inlays, crowns, veneers, and unit bridges. In order to be applied in oral environment, glass-ceramics are expected to show excellent aesthetic appearance and high strength besides acceptable chemical and wear resistance [4].

Among silicate ceramics, single chain silicates (like enstatite ($MgSiO_3$)), double chain silicates (like potassium fluorrichterite ($KNaCaMg_5Si_8O_{22}F_2$)), and multiple chain silicates (like fluorcanasite ($K_2Na_4Ca_5Si_{12}O_{30}F_4$)) perform excellent flexural strength and appropriate fracture toughness [5-7]. Fluorcanasite glass-ceramics present the morphology of randomly oriented interlocking blade-like crystals. These materials simultaneously present remarkable flexural strength (in the range of 200-300 MPa) and fracture toughness (about 3-5 $MPa.m^{1/2}$) [2, 8-13]. Nonetheless, chemical resistance of canasite glass-ceramics against acidic solutions is lower than soda lime silica glasses [14]. According to the international standard of dental ceramics (ISO 6872-2008), canasite glass-ceramics cannot be directly used in oral environment; hence their application has been restricted to the core material applications [15].

The term of canasite was firstly used by Dorfman in 1959 (and a subsequent paper in 1960). This monoclinic silicate material with chemical composition of $Ca_5(Na, K)_6Si_{12}O_{30}(OH, F)_4$ was found in Russia for the first time. In 1996, a similar material with triclinic structure was discovered in Yakutia and named frankamenite. However, according to the JCPDS database, this latter compound is usually reported as canasite-A [16, 17] The composition of fluorcanaite ($Ca_5Na_{3-4}K_{2-3}Si_{12}O_{30}F_4$) and frankamenite are very close to each other with different symmetries of monoclinic and triclinic crystalline structure [16, 18]. For this reason, the term of canasite is usually used to show simultaneous incidence of both fluorcanasite and frankamenite.

In the case of canasite glass-ceramic materials, existence of easy crystallographic cleavage sheets as well as anisotropic behavior of thermal expansion are known as the prominent toughening mechanisms [10, 11, 19, and 20]. Both factors induce crack deflection and micro-cracking effects [10]. These mechanisms will be intensified by the increase of aspect ratio and anisotropic orientations of canasite crystals in the microstructure [11, 21]. Due to superior mechanical properties and deep marble-like appearance, canasite-based glass-ceramic could be used as building materials in construction, as well [22]. Successful fabrication of these materials through concurrent sinter-crystallization procedure has been reported. Eilaghi *et al.* showed that partial replacement of Na_2O with K_2O in the parent glass could significantly improve sinterability and mechanical properties [23]. These characteristics also make canasite glass-ceramics attractive for use as magnetic memory disks [11, 14, and 24]. As reported in the literature, volume crystallization of canasite occurs through controlled two-step heat treatment of the parent glass. In the early steps of heat treatment (around 550-600°C), calcium fluoride (CaF_2) nucleates. By increase of temperature up to about 750-800°C, canasite starts to crystallize and grows on the calcium fluoride nuclei [25].

Several attempts have been focused on the improvement of chemical resistance of canasite glass-ceramics through modification of chemical composition of parent glasses [4, 26-31]. For the first time, Beall reported that addition of ZrO_2 develops fine-grained bodies with minimal fluoride content that improves whiteness and chemical resistance of the relevant glass-ceramics [9]. Anusavice and Zhang [26, 27], who studied the effect of Al_2O_3 additive on the canasite crystallization confirmed Improvement of chemical resistance. However, according to the dental ceramic standard (ISO 6872), the reported chemical durability was not satisfying enough for dental applications. Stokes *et al.* reported the mixed-alkali effect on chemical resistance of fluorcanasite glass-ceramics [28]. In this research, the best chemical resistance of fabricated glass-ceramics was obtained for the K7/Na8 composition ($60SiO_2$-$8Na_2O$-$7K_2O$-$15CaO$-$10CaF_2$). Pollington and Noort [2, 8] highlighted the role of ZrO_2 addition on

crystallization of fluorcanasite glass-ceramics. They reported biaxial flexural strength value of 250±26 MPa, fracture toughness of 4.2±0.3 MPa.m$^{1/2}$, and chemical solubility of 722±177 µg/cm^2. This class of fluorcanasite glass-ceramics has been utilized as the machinable ceramic core of resin-bonded veneers in restorative dentistry. The effect of different TiO_2 contents on crystallization trend of fluorcanasite glass-ceramics was monitored by Takav *et al.* [30]. It was reported that increase of TiO_2 in the composition suppressed crystallinity and deteriorated the interlocking status of canasite crystals resulting in the diminished mechanical properties.

According to previous research, addition of phosphorus oxide to the composition of glass can reduce viscosity of the molten silicate glasses [32]. Additionally, phosphorus oxide can intensify the possibility of phase separation, favor crystallization tendency and subsequently promote crystallinity of the final glass-ceramics [32-35]. Based on the mentioned points, the current work targets to elucidate the influence of P_2O_5 addition on crystallization, mechano-chemical properties and microstructural characteristics of canasite based glass-ceramics. It is worth mentioning that the previous research in this field had been mainly restricted to fabricate canasite glass-ceramics as bioactive materials for biomedical applications. Therefore, there is no in-depth research on the crystallization behavior and mechano-chemical characterization of P_2O_5 containing canasite glass-ceramics [3, 29, 36, 37]. Due to the significant similarity in chemical composition and structure of fluorcanasite and frankamenite, the term of canasite was jointly used to show simultaneous presence of these crystalline phases in this work. However, fluorcanasite and frankamenite were separately reported in such cases that they were distinguishable.

2. EXPERIMENTAL PROCEURES

The basic glass composition was chosen with respect to the stoichiometric composition of canasite, as given in Table 1. P_2O_5 containing glass compositions were also designed and labeled according to Table 1. To fabricate the starting glasses, reagent grade chemicals of Na_2CO_3, K_2CO_3, Ca_2CO_3, CaF_2, SiO_2 and P_2O_5

were used. The batches were transferred to the fused silica crucibles, and melted at 1350°C for 3 h. Afterwards, the obtained melts were quenched onto a preheated brass plate to produce glass ingots. Following this, the as-prepared glasses were immediately heat treated at 500°C for 1h in an annealing furnace to eliminate thermal history of glasses and probable internal stress.

Differential thermal analyzer (Bahr, STA503) was utilized to monitor crystallization behavior of the examined glasses. To this purpose, glass particles (0.5-0.6 mm) were analyzed by the DTA at 10°C/min heating rate. To exactly identify temperatures of T_g and T_d (respective glass transition and dilatometric softening point), glass pieces ($24 \times 5 \times 5$ mm^3) were subjected to the dilatometry test (DIL, 101-HT) with 10°C/min heating rate.

All glass specimens were heat treated through different procedures at the indicative temperatures taken from thermal analyses. In order to guarantee the amorphous inherence of the fabricated glasses and identification of crystalline phases developed during heat treatment, X-ray diffractometry was used. In this regard, powdered specimens were explored by the X-ray diffractometer (XRD, PhilipsPE3710) equipped with cupper lamp. The XRD patterns were obtained using 2θ ranging from 5° to 70°, then analyzed by diffraction software (PANalytical X'PERT PRO). Crystallinity degree of the glass-ceramic specimens was evaluated on the basis of Ohlberg-Strickler method in which the XRD data of specimens is required as equation (1) [38]:

$$X_c = (I_g - I_x)/(I_g - I_b) \times 100 \qquad (1)$$

Where I_g, I_x, I_b and X_c respectively refer to the intensity of the parent glass, intensity of the crystallized glass, intensity of mechanical mixture of initial raw materials, and the crystallinity degree of glass-ceramic specimen [38]. Cross sectional microstructures of the specimens were evaluated using a field emission scanning electron microscope (FESEM, Mira3 TESCAN) operating with the EDS detector (energy dispersive X-ray spectrometer) and elemental mapping analyzer. Before FESEM evaluations, the cross-sections of glass-ceramics were thoroughly polished, then immersed in 5 vol. % solution of hydrofluoric acid for chemical etching.

To determine chemical resistance of the glass-ceramic specimens, their chemical solubility was calculated based on the common standard of dental ceramics [15], following equation (2):

$$CS = (m_1 - m_2)/A^2 \qquad (2)$$

In this equation, $(m_1 - m_2)$, A^2, and CS accordingly show the weight loss (μg), surface area (cm^2), and chemical solubility (μg/cm^2). To measure chemical solubility, polished glass-ceramics were washed with deionized water, then dried for 4 h at 150°C. Afterwards, glass-ceramics were precisely weighed and soaked in dilute solution of acetic acid at 80°C for 16 h. Finally, the specimens were washed, dried and reweighed.

Mechanical properties of all glass-ceramic specimens were measured, precisely. Flexural strength was determined on the basis of three-point bending method [39]. The span length of 20 mm and the crosshead speed of 0.5 mm/min were used in this measurement. For each glass-ceramic series, a group of specimens with dimensions of $25 \times 5 \times 5$ mm^3 were used. Micro-hardness was evaluated according to the indentation method [40] using a Vickers indenter (Akashi, MVK-H21). The applied load of the diamond indenter (100 g) on the surface of specimens lasted for 15 s. Chantikul method [41] was applied to calculate fracture toughness (K_{IC}) of the glass-ceramic specimens. Flexural strength of the pre-cracked samples (applied load of 20 N for 15 seconds) was utilized to calculate the fracture toughness of samples following equation (3) [41]:

$$K_{IC} = 0.59(E/H)^{1/8} (\sigma P^{1/3})^{3/4} \qquad (3)$$

H, E, P and σ are related to the hardness, elastic modulus, the indentation load and flexural strength, accordingly. Based on the Chantikul report, the term of 0.59 $(E/H)^{1/8}$ section can be substituted with 0.88 [36].

Table 1. Chemical compositions of parent glasses (weight ratio).

Composition	SiO$_2$	K$_2$O	Na$_2$O	CaO	CaF$_2$	P$_2$O$_5$
Base	57.05	7.45	9.83	13.31	12.36	-
Base-P2	57.05	7.45	9.83	13.31	12.36	2
Base-P3	57.05	7.45	9.83	13.31	12.36	3
Base-P4	57.05	7.45	9.83	13.31	12.36	4
Base-P6	57.05	7.45	9.83	13.31	12.36	6

In order to quantify machinability of the examined specimens, brittleness index (B) was measured as equation (4) [42]:

$$B = \frac{H}{K_C} \qquad (4)$$

This parameter is given by the ratio of micro-harness (H) to fracture toughness (K_C). The more brittleness index means the less machinability.

3. RESULTS AND DISCUSSION

3.1. Thermal Analyses

Fig. 1 indicates DTA and dilatometry curves of the examined glasses. In the DTA curves, exothermic peaks indicate crystallization temperatures varying in the range of 635-790°C (see Fig. 1a). The identified crystallization peaks are different in multiplicity, intensity and temperature depending on the glass composition. In the DTA curve of the Base specimen, two minor and major crystallization peaks are detectable at 708 and 759°C, respectively. Slight increase of P_2O_5 in the Base-P2 specimen shifted both crystallization peaks to lower temperatures. However, crystallization peaks of other specimens backed to higher temperatures as the amount of P_2O_5 content further increased. The first crystallization peak of Base-P2

specimen locates at a very low temperature compared to other specimens. It seems that phase separation in the glass structure has developed the preferred crystallization sites for heterogeneous nucleation of CaF_2 crystallites at this temperature. Actually, in the presence of two glass network formers (SiO_2 and P_2O_5) in P_2O_5 containing glasses, the homogeneity of glass network is affected by the difference in the glass-forming ability (GFA) of the two glass network formers. Under these conditions, the instability of the glass may cause phase separation These separated zones contain specific elements (P- and Si-rich zones) that favor crystallization [33-35, 43]. It is worth mentioning that according to the previous research, precipitation of CaF_2 crystallites internally occurs at about 550°C. These crystallites act as the heterogeneous nucleating sites and favor the crystallization of canasite type phases at the second crystallization peak temperature [5, 9, 25, 44, 45].

As the amount of P_2O_5 increased further, the crystallization peak temperatures consequently increased. It seems that crystallization of a new phase at higher temperatures is responsible for the approximate increase of crystallization peak temperatures.
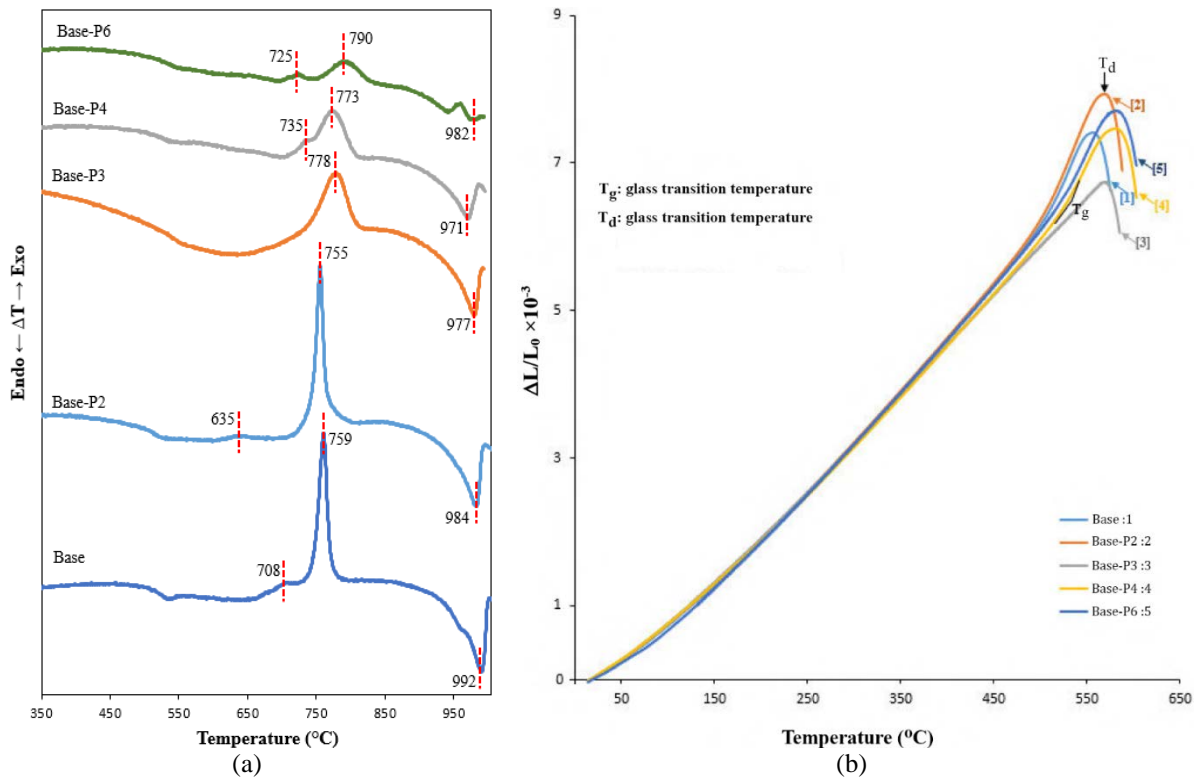

Fig. 1. a) DTA and b) dilatometry curves of parent glasses using the heating rate of 10°C/min.

Therefore, the higher amount of P_2O_5 means the higher crystallization peak temperatures of Base-P3, Base-P4, and Base-P6 specimens due to the consumption glass constituents needed for the precipitation of the new crystalline phase.

The typical temperatures of T_g (glass transition temperature) and T_d (dilatometric softening point temperature) were extracted from the dilatometry curves. In Table 2, the characteristic temperatures taken from DTA and dilatometry curves have been summarized. It is implied from Fig. 1b and Table 2 that continuing increase of P_2O_5 in the composition of parent glasses causes an increasing trend of T_g and T_d temperature. Increased values of T_g and T_d means that gradual increase of P_2O_5 enhances the glass viscosity. In addition, by gradual increase of P_2O_5 in the glass composition, thermal expansion coefficient follows a decreasing trend. Since thermal expansion behavior is restrained by the ability of glass network to collapse, glasses with higher network connectivity have a tendency to absorb thermal stress instead of thermal expanding. Therefore, gradual increase of P_2O_5 probably increases the glass network connectivity.

3.2. Development of Crystalline Phase

Fig. 2 depicts the XRD patterns of the specimens heat treated at the crystallization peak temperatures for 15 min using heating rate of 10°C/min. (Note that except Base-P3, other examined glasses have two crystallization peaks in the DTA curves.) According to Fig. 2, calcium fluoride (CaF_2- JCPDS 65-535) crystallizes at the first crystallization peak of each specimen. Additionally, slight peak lines of fluorcanasite $((Na, K)_6Ca_5Si_{12}O_{30}(OH, F)_4$- JCPDS 13-553), frankamenite $((Na_3K_3Ca_5Si_{12}O_{30}F_3(OH).H_2O)$- JCPDS 45-1398) and fluorapatite $((Ca_5FO_{12}P_3)$- JCPDS 76-558) can be detected in some specimens heat treated at first peak temperature. As shown in Fig. 2, with further enhancement of temperature to the next crystallization peak, fluorcanasite and frankamenite phases appear as the main crystalline phases. However, fluorapatite, fluorcanasite and frankamenite precipitate more effectively at the second crystallization peak temperature of P_2O_5 containing glasses. By increase of P_2O_5 content, the number and intensity of fluorapatite peak lines slightly increase.

It is noticeable that the peak line intensities of fluorcanasite and frankamenite have been diminished in the P_2O_5 containing glass-ceramics, probably due to the concurrent crystallization of fluorapatite along with these phases. In other words, precipitation of fluorapatite consumes the constituents which are needed for consequent crystallization of fluorcanasite and frankamenite crystalline phases. As mentioned earlier, this phenomenon could be responsible for the increasing of crystallization peak temperatures of P_2O_5 containing specimens. After identification of crystallized phases developed at the crystallization temperatures, all parent glasses were separately subjected to the two-step (nucleation and growth) heat treatment. For each glass, the average of T_g and T_d was set as the nucleation temperature; while the main crystallization peak temperature in each DTA curve was selected as the growth temperature.

Table 3 summarizes all heat treatment schedules applied to the examined glasses. Afterwards, XRD patterns were prepared from all glass-ceramics subjected to the two-step heat treatment. As shown in Fig. 3, the main crystalline phases in all glass-ceramic specimens are fluorcanasite and frankamenite. Fluorapatite is also observable in the P_2O_5 containing glass-ceramics. It is implied from Fig. 3 that all peak lines have been declined in the XRD pattern of Base-P2 specimen, and then enhanced significantly with further increase of P_2O_5. The total decrease in intensity of Base-P2 may be originated from consumption of glass components to form a new phase (fluorapatite) in this specimen.

Table 2. Characteristics temperatures extracted from DTA and dilatometry curves besides thermal expansion coefficients.

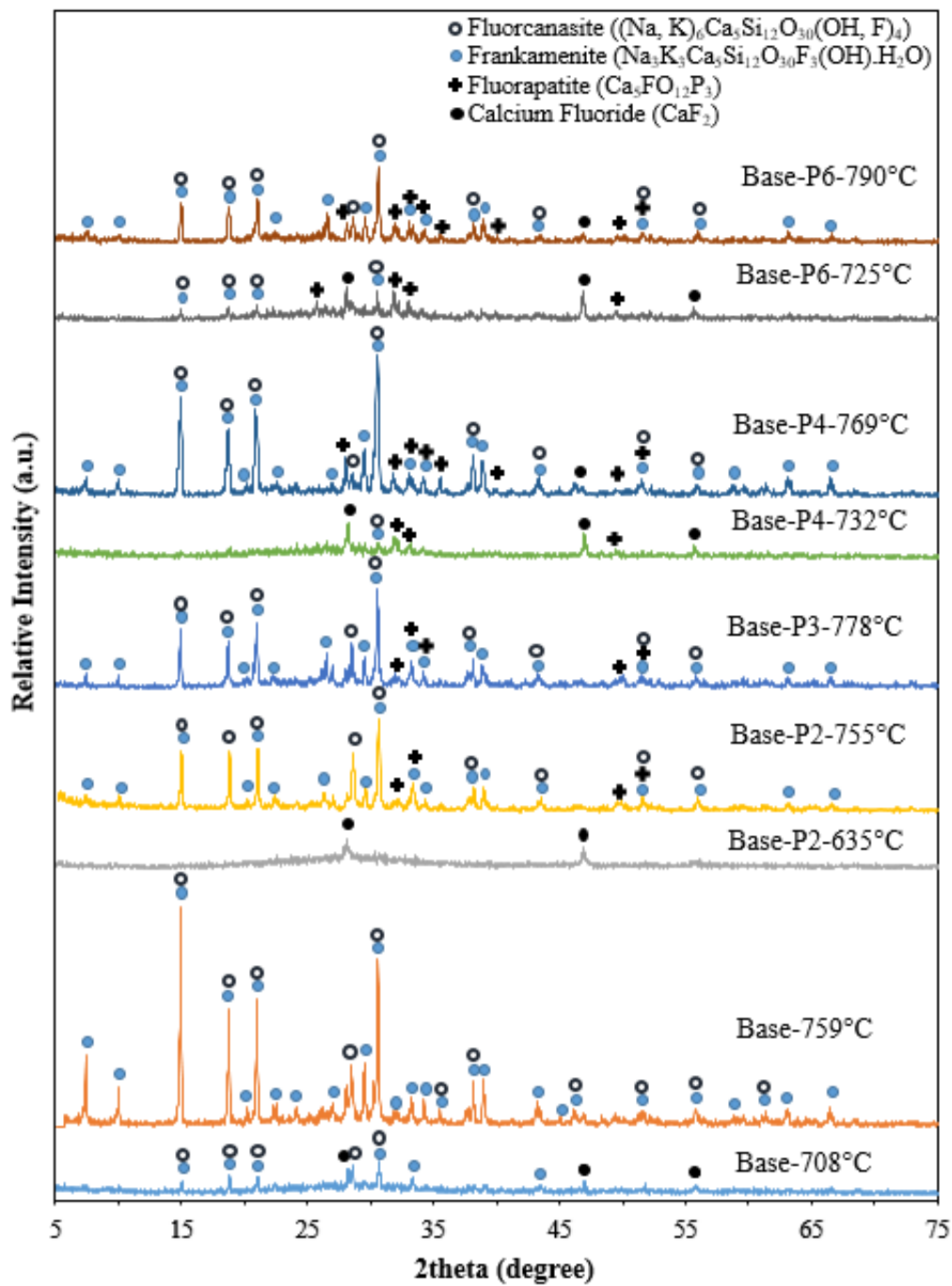| Glass	T_g (°C)	T_d (°C)	T_{c1} (°C)[a]	T_{c2} (°C)[b]	$\alpha \times 10^{-6}$ (1/K) (35-500 °C)
Base	514	556	708	759	12.94
Base-P2	521	569	635	755	13.09
Base-P3	541	569	-	778	12.33
Base-P4	533	581	732	769	12.51
Base-P6	539	581	725	790	12.86
[a] T_{c1}: temperature of the first crystallization peak, [b] T_{c2}: temperature of the second crystallization peak,					

Fig. 2. X-ray diffraction patterns of the glasses subjected to the one-step heat treatment at the crystallization peak temperatures for 15 min.

Table 3. Two step heat treatment schedules applied to the examined glasses.

Glass	heating rate (°C/min)	Nucleation temperature (°C)/ holding time (h)	Growth temperature (°C)/ holding time (h)
Base	10	535/2	759/2
Base-P2	10	545/2	755/2
Base-P3	10	555/2	778/2
Base-P4	10	557/2	769/2
Base-P6	10	560/2	790/2
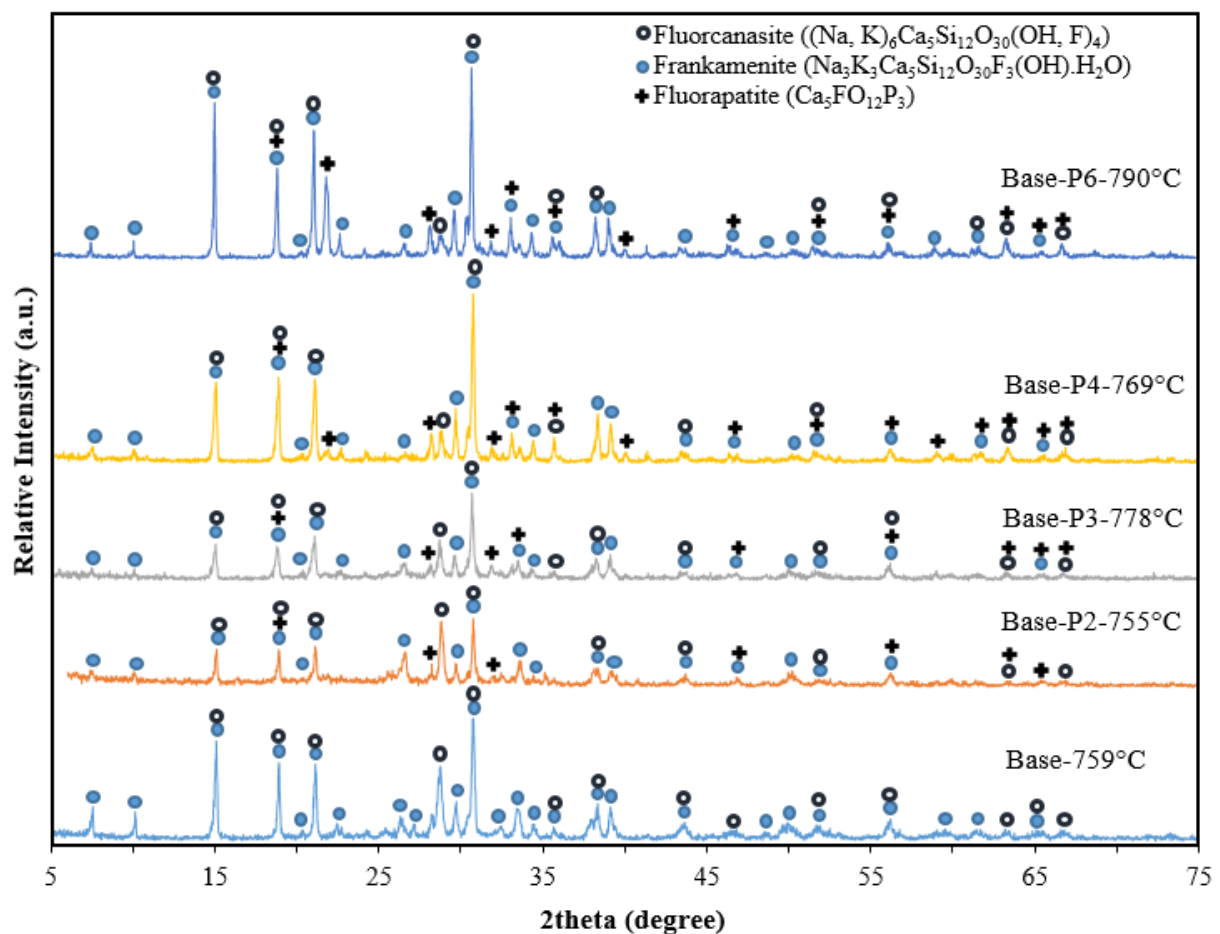
Fig. 3. X-ray diffraction patterns of the glass-ceramics treated using a two-step heating procedure.

According to the JCPDS 45-1398 reference, the major XRD peak line of frankamenite locates at $2\theta= 30.6$. As the amount of P_2O_5 increases up to 6 weight ratio, this peak line intensifies. Furthermore, the number and intensity of fluorapatite peak lines raise significantly by the increase of P_2O_5 content. This means that a much higher level of frankamenite and fluorapatite crystalline phases is formed. In other words, addition of P_2O_5 to the glass composition has probably facilitated the crystallization of frankamenite and fluorapatite phases. On the other hand, the peak line located at $2\theta= 28.6$ (according to JCPDS 13-0553) could be considered as the discriminating line of fluorcanasite. Since this peak line is significantly declined by further increase of P_2O_5, it seems that crystallization of fluorcanasite is restricted in the P_2O_5 containing glass-ceramics. Referring to the XRD patterns of Fig. 3, it can be concluded that the Base-P2 glass-ceramic illustrates the weakest peak line at $30.6\ 2\theta$ as well as the strongest peak line at $28.6\ 2\theta$ compared to other glass-ceramic specimens. This means that the highest amount of fluorcanasite and the lowest amount of frankamenite phase develop out of all glass-ceramic specimens in the Base-P2 glass-ceramic. The crystallization tendency of all glass-ceramic specimens was evaluated on the basis of Ohlberg-Strickler equation [33]. This evaluation was carried out using an average value of ten 2θ for each glass-ceramic. According to the obtained results (see Table 4), gradual modification of glass composition with P_2O_5 slightly increases the crystallinity values. This effect will be discussed in the next parts.

3.3. Microstructural Observations

To assess the possibility of phase separation in the studied glasses, they were treated at nucleation temperature for 2 h, then examined by XRD analysis. Fig. 4 shows the FESEM images of the examined glasses. All glasses indicate phase separated structures in which spherical droplets are homogeneously dispersed in the glass matrix.

This type of structure is in accordance with the typical nucleation and growth mechanism of phase separation [22, 46]. However, based on the XRD patterns of Fig. 5 partial crystallization occurs in the P_2O_5 containing specimens. It is believed that occurrence of phase separation aids crystallization process, thermodynamically and kinetically through developing appropriate nucleating sites and decreasing the diffusion path between the constituents of newly crystallized phases in the separated areas [46]. Therefore, it seems that the intensified phase separation is responsible for favored crystallization of P_2O_5 bearing specimens.

Table 4. Crystallinity degree of the fabricated glass-ceramics.

Glass-ceramic	Base	Base-P2	Base-P3	Base-P4	Base-P6
X_c (Crystallinity degree)	84.90	84.11	85.79	88.09	90.04

a

b

c

d

e
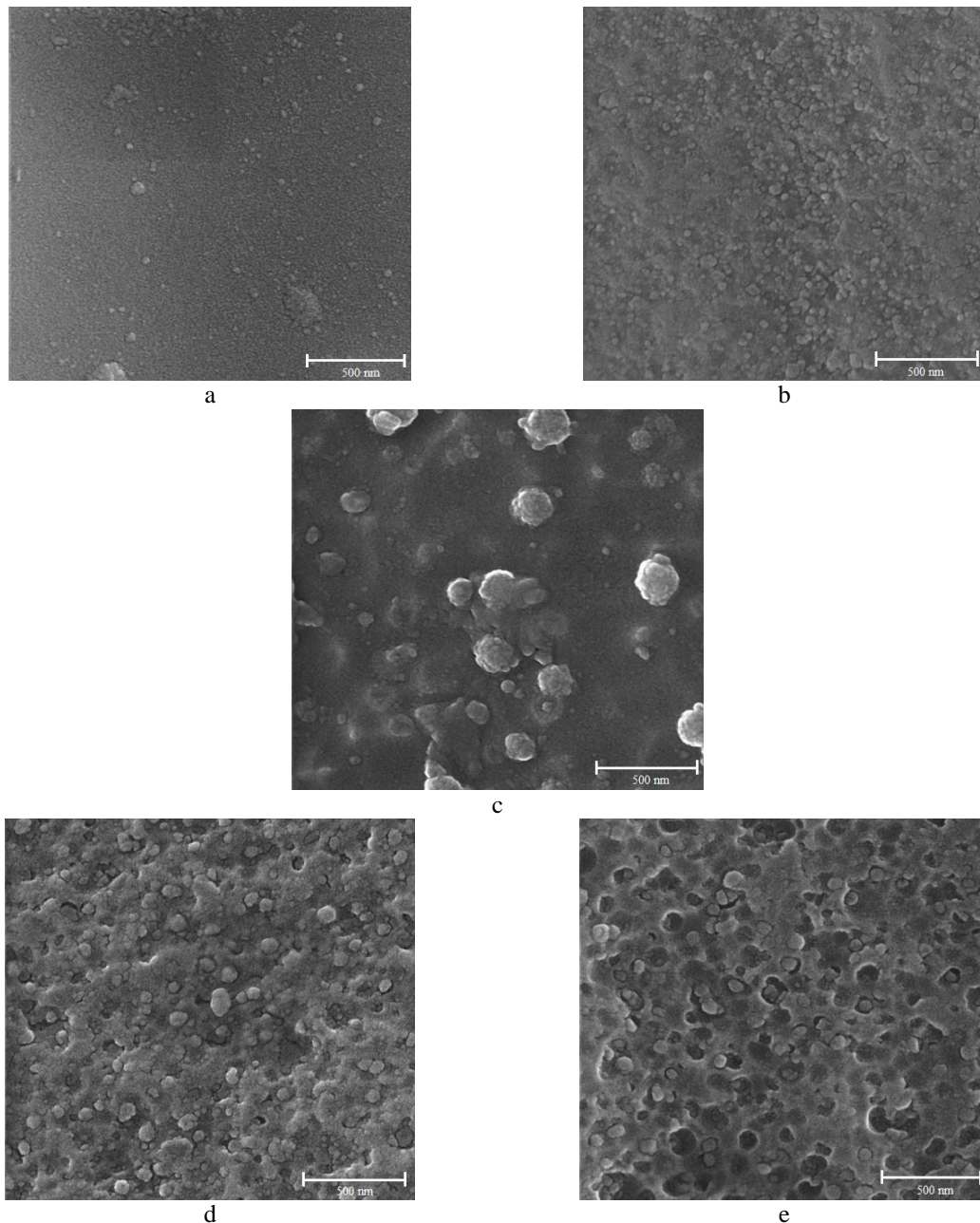
Fig. 4. FESEM images illustrating the microstructure of chemically etched glasses heat treated at nucleation temperature for 2 hours: a) Base, b) Base-P2, c) Base-P3, d) Base-P4, and e) Base-P6.
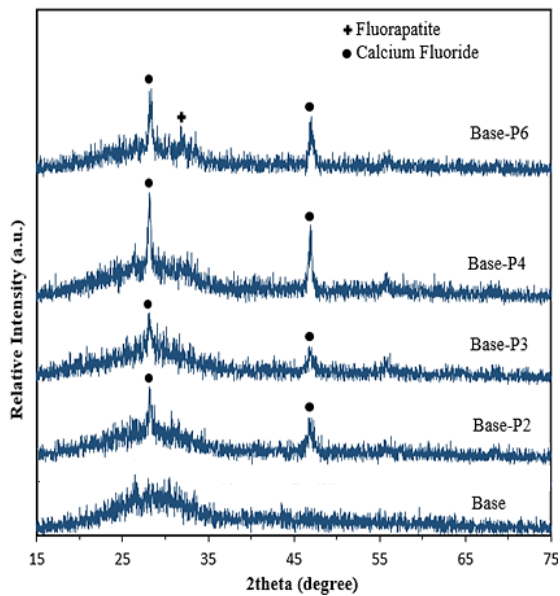
Fig. 5. X-ray diffraction patterns of specimens undergone heat treatment at nucleation temperatures for 2 hours.

The FESEM images taken from chemically etched cross sections of the two-step heat treated samples along with the EDS spectra taken from crystalline phases can be observed in Figs. 6-10. On the basis of microstructural evaluations, randomly oriented crystals with the blade-like morphology are detectable at different levels of magnification in all examined glass-ceramics. According to the EDS analyses (Figs. 6c, 7d, 8d, 9d and 10d), these crystals have canasite inherence but it is not possible to discriminate fluorcanasite from frankamenite due to the very close chemical composition of these crystalline phases. Additionally, submicron pseudo-spherical crystals cab be observed in the microstructure of P_2O_5 containing glass-ceramics at higher magnifications. Considering very small size of these spherical crystals, it is not possible to exactly determine their chemical composition. However, considering significant amounts of calcium, phosphorous, and fluoride ions in the EDS spectra (see Figs. 7e, 8e, 9e, and 10e), they can be assigned to fluorapatite.
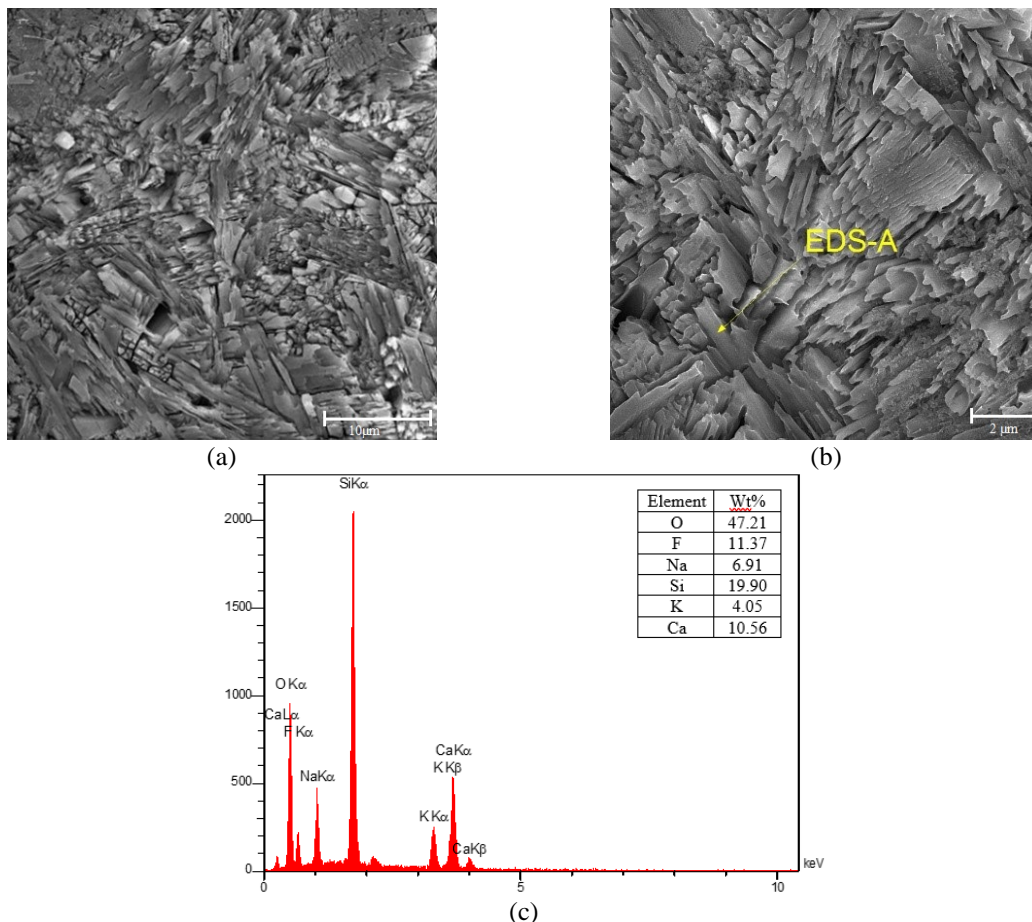

Fig. 6. FESEM images capturing the microstructure of the Base glass-ceramic at various magnification levels: a) 5000, b) 15000, and c) the EDS spectrum of zone A.
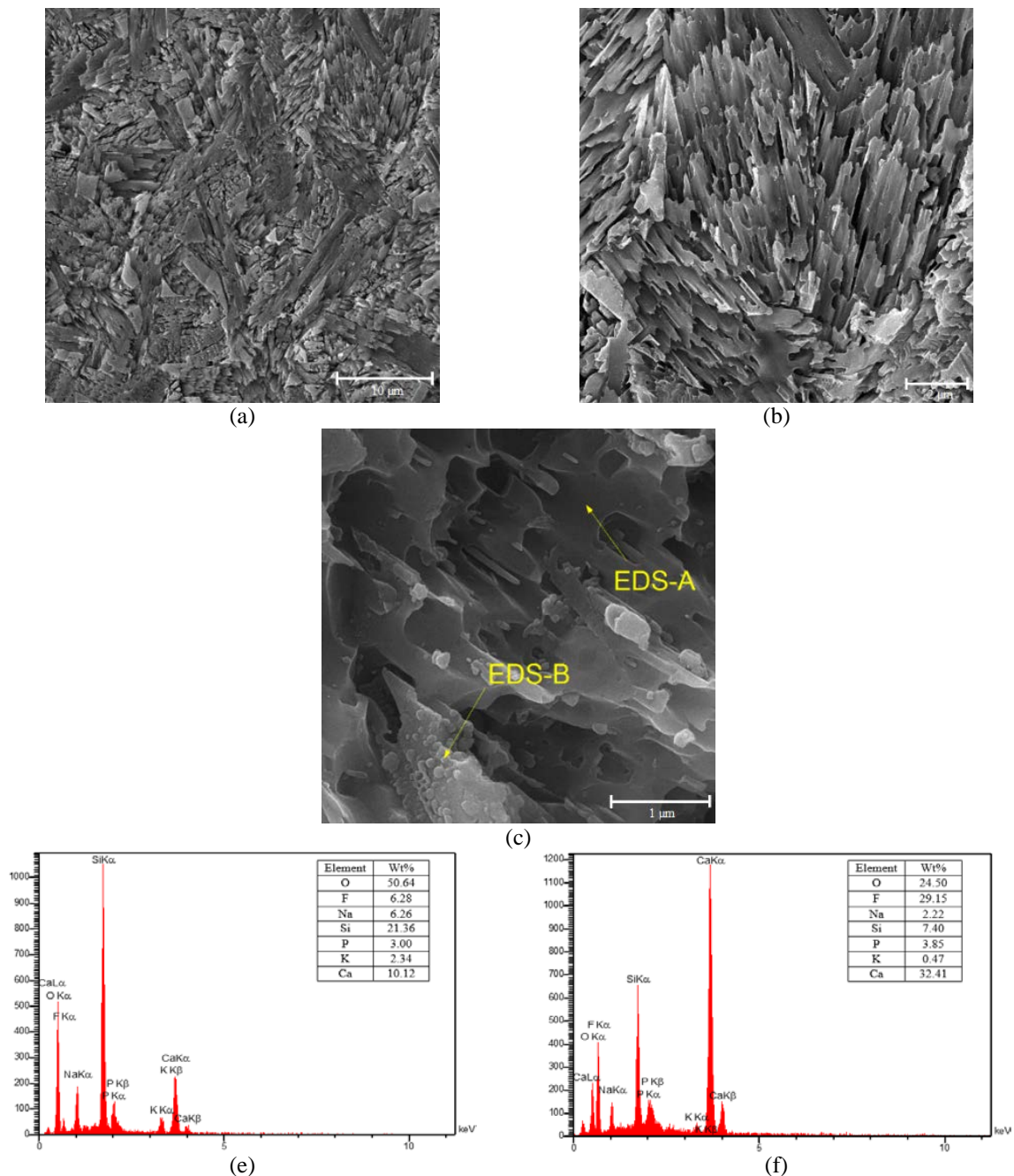
(a)

(b)

(c)

(e)

(f)

Fig. 7. FESEM images capturing the microstructure of the Base-P2 glass-ceramic at various magnification levels: a) 5000, b) 15000, c) 50000, and the EDS spectra of d) zone A, and e) zone B.

It is also evident from FESEM observations that the blade-like crystals of canasite (fluorcanasite and frankamenite) have lost the interlocked orientation and grown in one direction in P_2O_5 containing glass-ceramics. On the other hand, the blade-like crystals are lager in size in the high P_2O_5 content glass-ceramics in comparison with the Base and Base-P2 glass-ceramics. This microstructural coarsening besides changing canasite morphology from randomly interlocked orientation to one dimensional growth originate from crystallization of fluorapatite in the corresponded glass-ceramics. Actually, by crystallization of fluorapatite in the P_2O_5 containing glass-ceramics, the concentration of required constituents for crystallization of canasite type phases is diminished. As a result, the number of canasite crystals decreases and the given thermal energy during heat treatment favors the one-dimensional growth of large crystals.
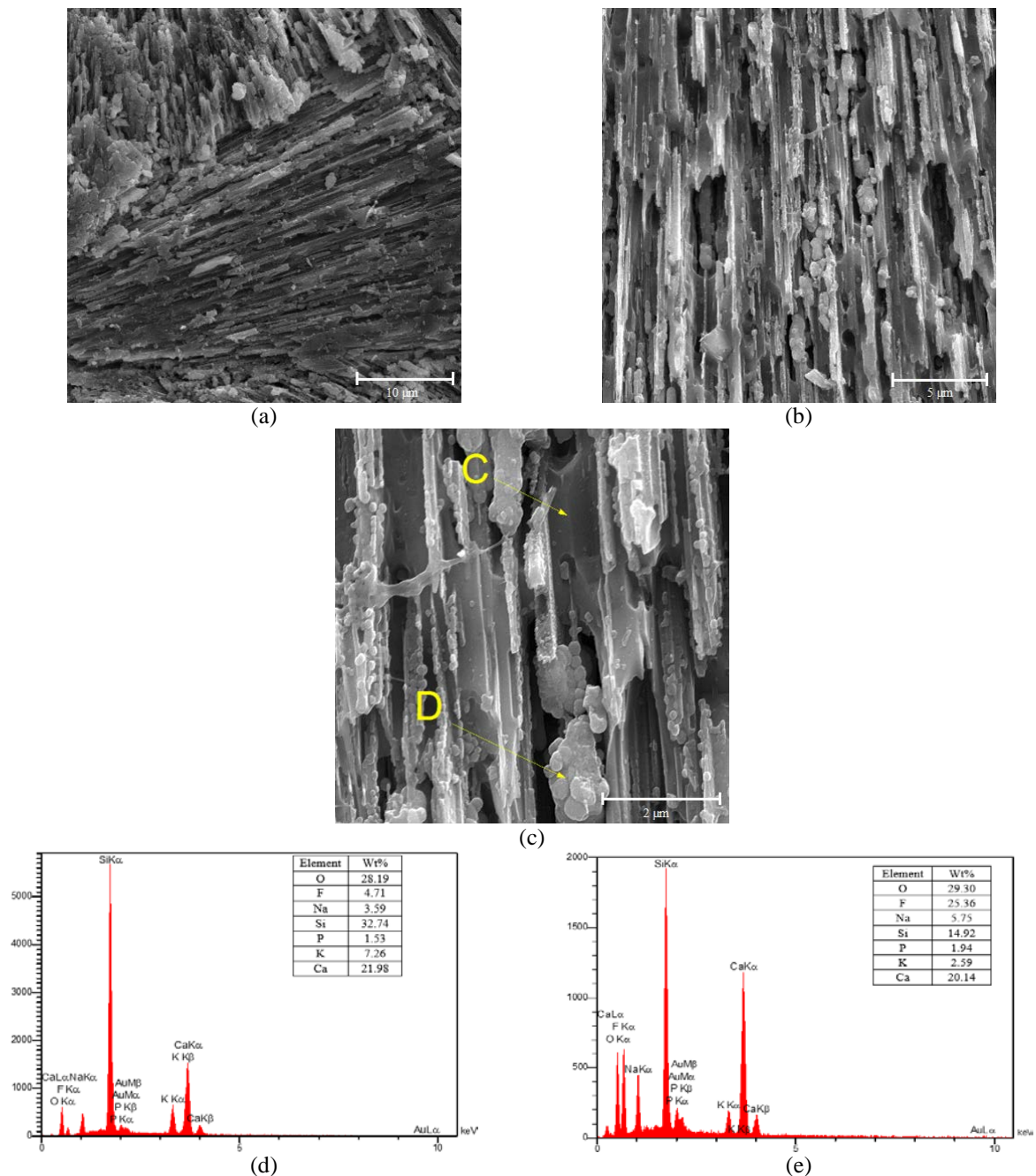
Fig. 8. FESEM images capturing the microstructure of the Base-P3 glass-ceramic at various magnification levels: a) 5000, b) 10000, c) 30000, and the EDS spectra of d) zone C, and e) zone D.

3.4. Mechanical and Chemical Performance

Mechanical features besides chemical solubility of the glass-ceramics prepared trough two-step heat treatment were measured. These measurements have been presented in Fig. 11. The measured values of chemical solubility indicate that the Base-P3 and Base-P6 glass-ceramics have the best and the worst chemical resistance, respectively. It is noticeable that chemical resistance of glass-ceramics depends on

several parameters including chemical durability of crystallized phases, volume fraction of each crystalline phase, chemical composition of the residual glass phase as well as the extension of crystal glass interfaces. About Base and Base-P2 specimens, the smaller crystal size and finer microstructure has led to increase of interphase boundaries that are weak areas against chemical attack. Therefore, the Base-P3 specimen with coarser microstructure indicates less chemical

solubility in comparison with the other glass-ceramics. On the other hand, by further increase of P_2O_5 in the glass composition phase separation has been intensified, consequently.

It is known that phase separated glasses are more susceptible to chemical corrosion due to the increased chemical solubility of some separated areas being rich of alkaline and alkaline earth ions. Therefore, chemical solubility of Base-P4 and Base-P6 (with higher glass phase separation tendency) glass-ceramics drastically increases.

In view point of mechanical properties, the Base-P2 glass-ceramic demonstrates the highest flexural strength and fracture toughness among all examined glass-ceramics. As discussed previously, this glass-ceramic shows randomly interlocked orientation of crystalline phases that guarantees suitable mechanical properties. Such morphology causes crack deflection, which is the main mechanism for strengthening and toughening of specimen [11, 47].
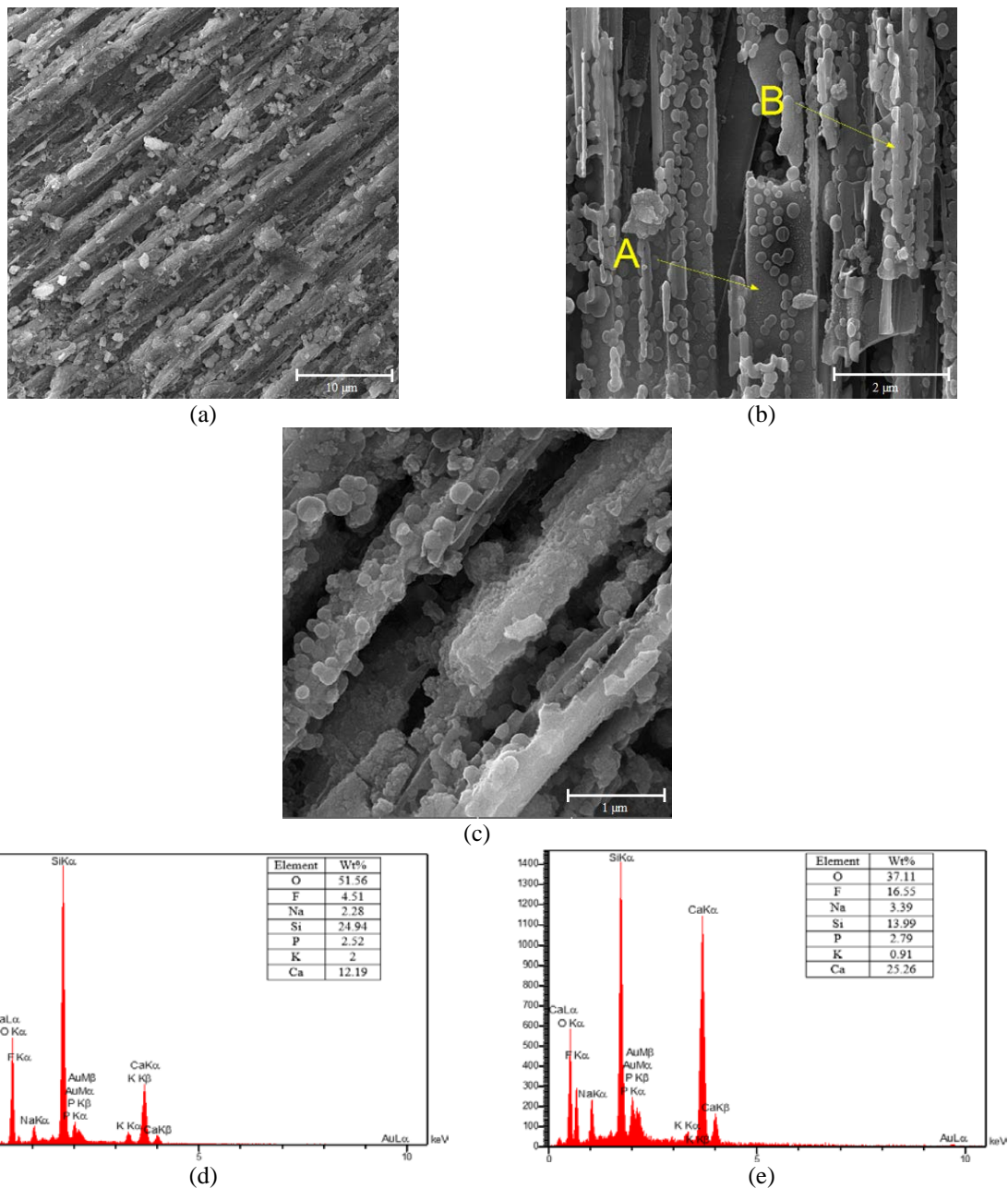

(a)

(b)

(c)

(d)

(e)

Fig. 9. FESEM images capturing the microstructure of the Base-P4 glass-ceramic at various magnification levels: a) 5000, b) 30000, c) 50000, and the EDS spectra of d) zone A, and e) zone B.
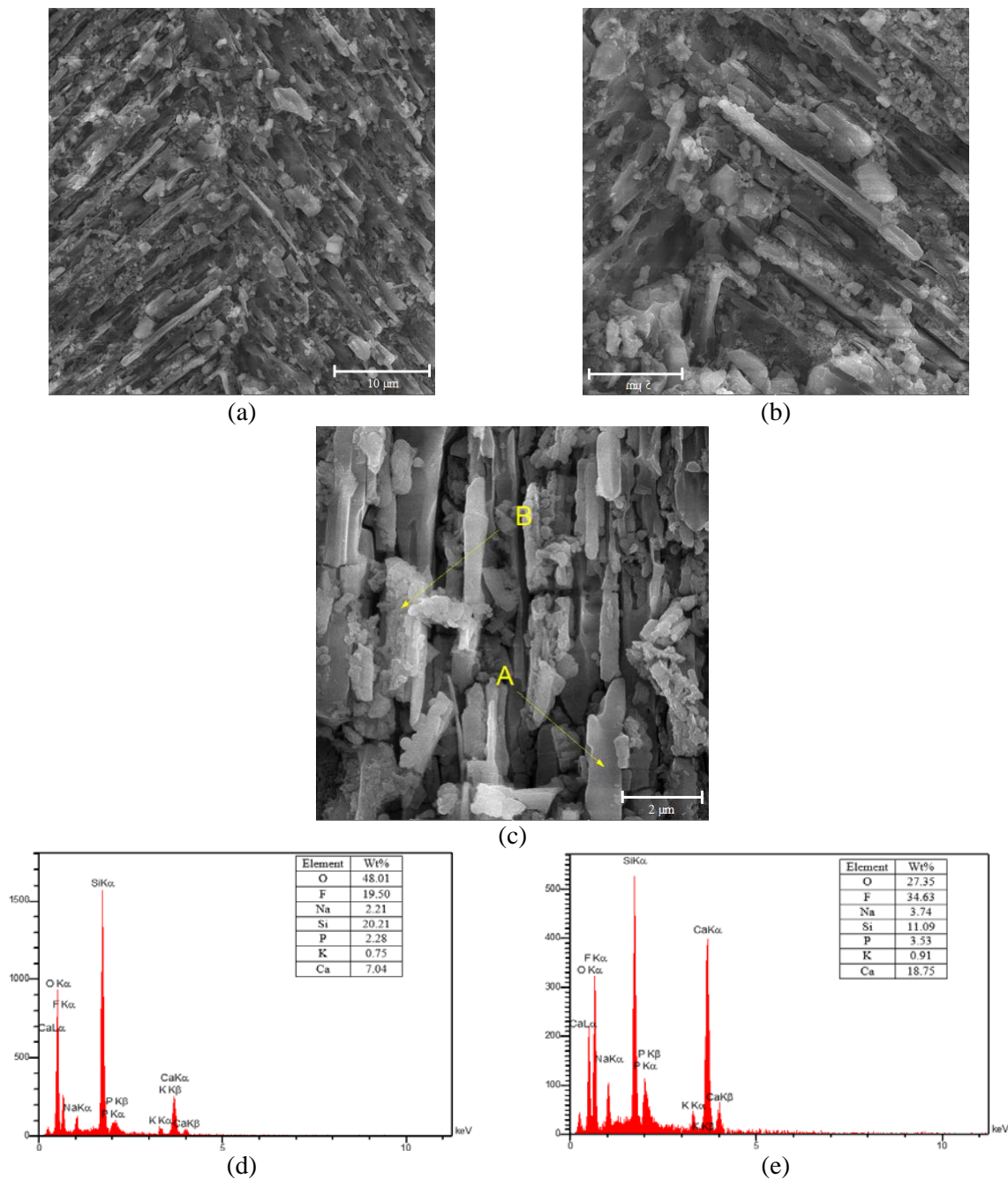
(a)

(b)

(c)

(d)

(e)

Fig. 10. FESEM images capturing the microstructure of the Base-P6 glass-ceramic at various magnification levels: a) 5000, b) 10000, c) 20000, and the EDS spectra taken from d) zone A, and e) zone B.

Regardless of the above-mentioned parameters, Base-P2 glass-ceramic has the highest amount of fluorcanasite along with the lowest amount of frankamenite compared to other specimens as shown in Fig. 4. According to the previous research conducted by Rozhdestvenskaya *et al.* [48], the crystal lattice of frankamenite phase is weakened due to the dominance of F$^-$ ions over OH$^-$ groups. In other words, more groups of OH$^-$ in the fluorcanasite phase fixate the structure of the glass-ceramic through more hydrogen bonds between the silicate chains and the octahedral occupied ions. Totally, it can be concluded that finer microstructure with interlocked oriented crystal morphology as well as higher amount of fluorcanasite are responsible for the improved flexural strength and fracture toughness of Base-P2. Referring to ISO 6872 [15], the flexural strength less than 100 MPa is not acceptable for restorative dental cores. Therefore, glass-

ceramics containing more than 2 weight ratios of P_2O_5 cannot fulfill the mechanical requirements for this application.

Considering Fig. 11, Vickers micro-hardness is moderately influenced by the glass composition, except Base-P6. This specimen has the least value of micro-hardness due to the effective crystallization of fluorapatite.

Among all examined specimens, Base and Base-P2 indicate the least values of brittle index. This parameter is defined as quantitative evidence for machinability of materials. According to the relevant standard, the maximum acceptable brittleness index for suitable machining of glass-ceramic materials is 4.3 $\mu m^{-1/2}$ [49]. Considering the measurements of both mechanical and chemical properties, Base-P2 was selected as the most favorable glass-ceramic. In order to qualitatively assess machinability, this glass-ceramic was machined and perforated using CNC machine and cobalt drill (1.5 mm), respectively. Fig. 12 shows the optical microscopy image taken from a piece of machined and drilled Base-P2 glass-ceramic.
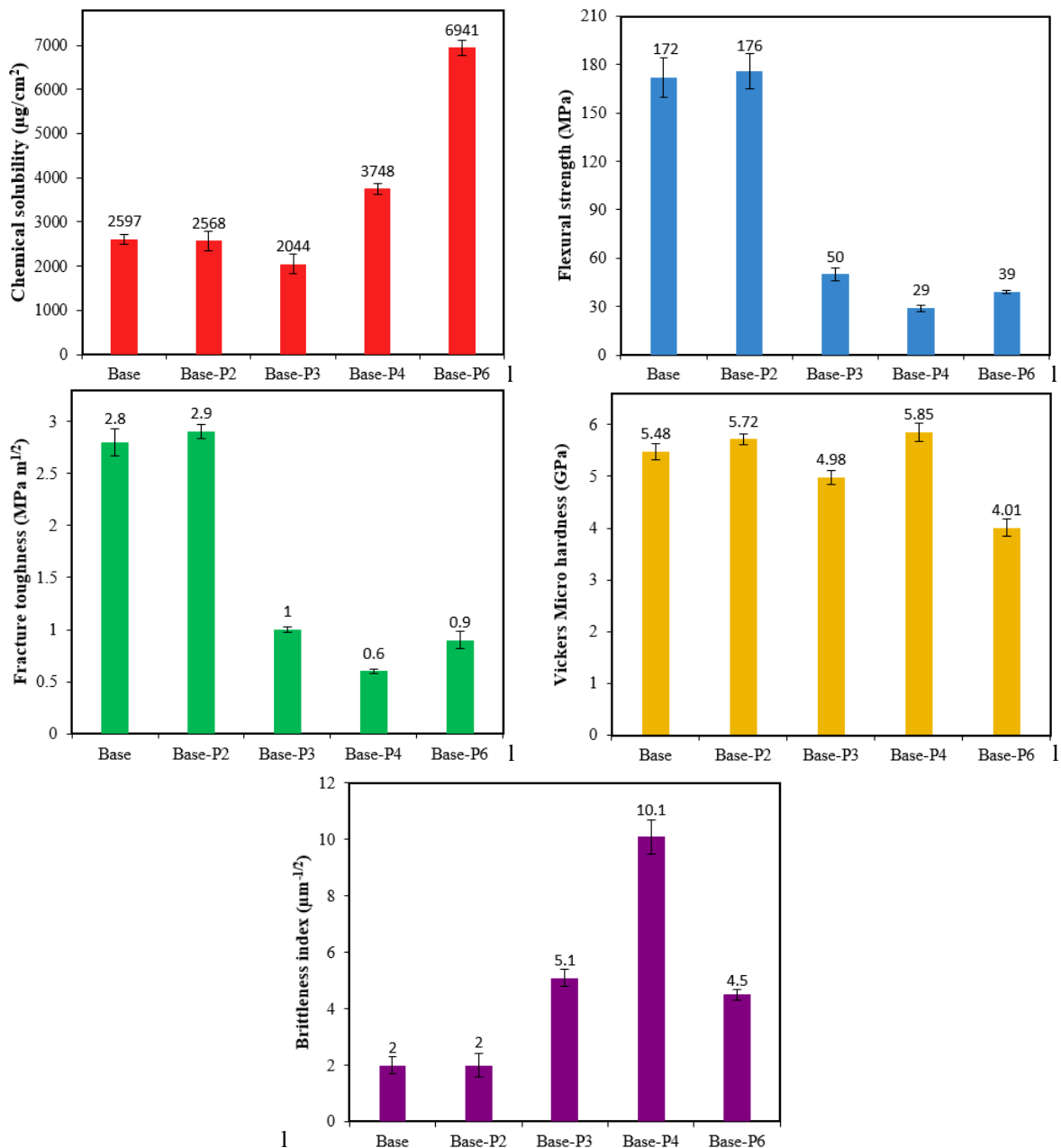

Fig. 11. Mechanical and chemical performance of the glass-ceramics after undergoing a two-step heat treatment.

This specimen appeared without any fracture or surface chipping after machining. The drilled hole was also created in the whole depth of the specimen without any obvious deviation or crack.
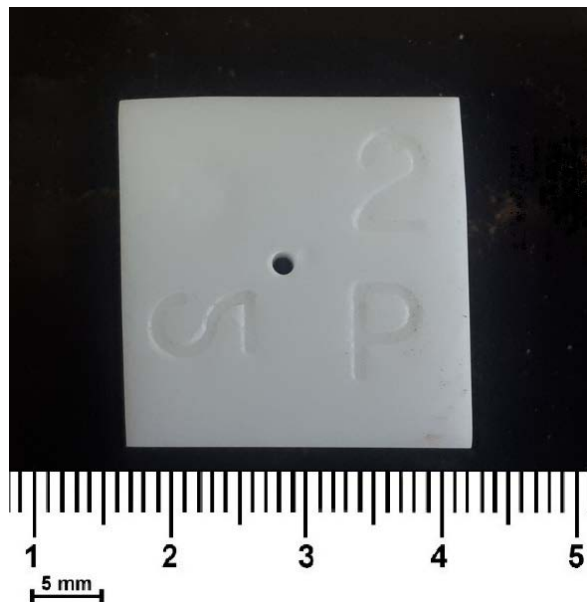

Fig. 12. Optical microscopy image of mechanically machined and holed Base-P2 glass-ceramics.

4. CONCLUSIONS

In the present work, two-step heat treatment procedures were employed to prepare canasite based glass-ceramics from parent glasses containing different amounts of P_2O_5. The main crystalline phases in all specimens were fluorcanasite and frankamenite. The fluorapatite phase was also identified in the P_2O_5 bearing glass-ceramics. Addition of P_2O_5 to the basic composition of glass and its further enhancement led to intensify liquid-liquid type phase separation in starting glasses and also promoted crystallinity of the corresponded glass-ceramics. According to the microstructural survey, canasite and fluorapatite were randomly interlocked in the shape of blades and sphers, respectively. However, by further addition of P_2O_5 randomly orientation of canasite crystals deteriorated and they grew in one direction. Within the analyzed specimens, Base-P2 had the highest flexural strength (176 MPa) as well as fracture toughness (2.9 MPa.m$^{1/2}$) and the least value of brittle index (2 μm$^{-1/2}$). Chemical resistance of this glass-ceramic was obtained about 2000 mg/cm^2, being acceptable for core dental restorations according to the ISO 6872. This specimen appeared without

any fracture or surface chipping after machining. Therefore, it could be candidate as the core material in restorative dentistry.

REFERENCES

[1].   Montazerian, M. and Zanotto, E. D., "Bioactive and inert dental glass-ceramics", J. Biomed. Mater. Res. Part A, 2016, 105, 619-639.

[2].   Pollington, S. and Van Noort, R., "Manufacture, characterization and properties of novel fluorcanasite glass-ceramics", J. Dent., 2012, 40, 1006-1017.

[3].   Ghosh, S. B., Reaney, M., Brook, M., Gillingham, K. H., Johnson, A. and Hatton, P. V., "In vitro biocompatibility of fluorcanasite glass-ceramics for bone tissue repair", J. Biomed. Mater. Res. Part A, 2006, 80, 175-183.

[4].   Deng, W., Cheng, J. S., Tian, P. J. and Wang, M. T., "Chemical durability and weathering resistance of canasite based glass and glass-ceramics", J. Non-Cryst. Solids, 2012, 358, 2847-2854.

[5].   Likitvanichkul, S. and Lacourse, W. C.,"Effect of fluorine content on crystallization of canasite glass-ceramics", J. Mater. Sci., 1995, 30, 6151-6155.

[6].   Geng, X., Zhu, Z., Cao, J., Wang, Z., Lu, J. and Qian, G., "Non-equilibrium cooling regulating and crystallization of canasite-A glass-ceramics from high sodium solar silicon waste slag", Ceram. Int., 2021, 47, 13874-13883.

[7].   Geng, X., Cao, J., Wang, Z. and Lu, J., "Selective controlled precipitation mechanism of canasite and xonotlite glass-ceramics from silica slag", J. Non-Cryst. Solids, 2020, 546, 120283.

[8].   Pollington, S., Fabianelli, A. and Van Noort, R., "Microtensile bond strength of a resin cement to a novel fluorcanasite glass-ceramic following different surface treatments", J. Dent. Mater., 2010, 26, 864-872.

[9].   Beall, G., Alkali metal, calcium fluorosilicate glass-ceramics, USPatent 4386162, 1983.

[10].   Johnson, A., Shareef, M. Y., Van Noort, R. and Walsh, J. M., "Effect of furnace type and ceramming heat treatment conditions

on the biaxial flexural strength of a canasite glass-ceramic", Dent. Mater., 2000, 16, 280-284.

[11]. Holand, W. and Beall, G., Glass-Ceramic Technology, New Jersey, USA, 2002, 147-148.

[12]. Ghosh, S. B., Reaney, I. M., Johnson, A., Brook, I. M., Gillingham, K. H. and Hatton, P. V., "Castability and, biocompatibility of novel fluorcanasite glass-ceramics", Key Eng. Mater., 2006, 309-311, 293-296.

[13]. Farag, M. M., El-Rashedi, A. M. I. and Russel, C., "In vitro biocompatibility evaluation of canasite-calcium phosphate glass-ceramics", J. Non-Cryst. Solids, 2018, 488, 24-35.

[14]. Omar, A. A., Hamzawy, E. M. A. and Farag, M. M.,"Crystallization of fluorcanasite- fluorrichterite glasses", Ceram. Int., 2009, 35, 301-307.

[15]. ISO 6872: 2008 (E), Dentistry-Ceramic Materials.

[16]. Khomyakov, A. P., Nechelyustov, G. N., Krivokoneva, G. K., Rastsvetaeva, R. K., Rozenberg, K. A. and Rozhdestvenskaya, I. V., "Fluorcanasite, $K_3Na_3Ca_5Si_{12}O_{30}(F,OH)_4.H_2O$, a new mineral species from the Khibiny alkaline pluton, Kola Peninsula, Russia, and new data on canasite", Geol. Ore Deposits, 2009, 51, 757-766.

[17]. Miller, C. A., Reaney, I. M., Hatton, P. V. and James, P. F., "Crystallization of canasite/frankamenite-based glass-ceramics", Chem. Mater., 2004, 16, 5736-5743.

[18]. Beall, G. H., "Chain silicate glass-ceramics", J. Non-Cryst. Solids, 1991, 129, 163-173.

[19]. Pollington, S., "Novel glass-ceramics for dental restorations", J. Contemp. Dent. Pract., 2011, 12, 60-67.

[20]. Beall, G. H., CHyung, K., Stewart, R. L., Donaldson, K. Y., Lee, H. L., Baskaran, S. and Hasselman, D. P. H., "Effect of test method and crack size on the fracture toughness of a chain-silicate glass-ceramic", J. Mater. Sci., 1986, 21, 2365-2372.

[21]. Oguma, M., Chyung, K., Donaldson, K. Y. and Haselman, D. P. H., "Effect of crystallization on thermal shock behavior of a chain-silicate canasite glass-ceramic", J. Amer. Ceram. Soc., 1987, 70, C2-C3.

[22]. Deng, W., Gong, Y. and Cheng, J., "Liquid-phase separation and crystallization of high silicon canasite-based glass ceramic", J. Non-Cryst. Solids, 2014, 385, 47-54.

[23]. Eilaghi, M., Montazerian, M. and Eftekhari Yekta, B., "Effect of partial substitution of K_2O for Na_2O on sintering, crystallization and mechanical properties of SiO_2-CaO-K_2O-Na_2O-CaF_2", Trans. Ind. Ceram. Soc., 2016, 75, 1-6.

[24]. Beall, G. H., "Design and properties of glass-ceramics", Annu. Rev. Mater. Sci., 1992, 22, 91-119.

[25]. Oh, W., Zhang, N. and Anusavice, K. J., "Effect of heat treatment on fracture toughness (KIC) and microstructure of a fluorcanasite-based glass-ceramic", J. Prosthodontics, 2007, 16, 439-444.

[26]. Anusavice, K. J., and Zhang, N. Z. "Chemical durability of Dicor and fluorcanasite-based glass-ceramics", J. Dent. Res., 1998, 77, 1553-1559.

[27]. Zhang, N. and Anusavice, K. J., "Effect of alumina on the strength, fracture toughness, and crystal structure of fluorcanasite glass-ceramics", J. Am. Ceram. Soc., 1999, 82, 2509-2513.

[28]. Stokes, C. W., Van Noort, R. and Hand, R. J., "Investigation of the chemical solubility of mixed-alkali fluorcanasite forming glasses", J. Non-Cryst. Solids, 2006, 352, 142-149.

[29]. Kanchanarat, N., Ghosh, S. B., Reaney, I. M., Brook, I. M. and Hatton, P. V., "Microstructure and mechanical properties of fluorcanasite glass-ceramics for biomedical applications", J. Mater. Sci., 2008, 43, 759-765.

[30]. Takav, P., Banijamali, S., Hossein Zadeh, A. S. A. and Mobasherpour, I., "Influence of TiO_2 content on phase evolution, microstructure and properties of fluorcanasite glass-ceramics prepared through sintering procedure for dental restoration applications", Ceram. Int., 2018, 44, 7057-7066.

[31]. Shamohammadi Ghahsareh, Z., Banijamali, S. and Aghaei, A., "Cerium

oxide containing canasite based glass-ceramics for dental applications: Crystallization behavior, mechanical and chemical properties", Ceram. Int., 2022, 48, 8489-8501.

[32]. Xiao, Z., Zhou, J., Wang, Y. and Luo, M., "Microstructure and properties of Li_2O-Al_2O_3-SiO_2-P_2O_5 glass-ceramics", Open Mater. Sci., 2011, 5, 45-50.

[33]. Tulyaganov, D. U., Agathopoulos, S., Ventura, J. M., Karakassides, M. A., Fabrichnaya, O. and Ferreira, J. M. F., "Synthesis of glass-ceramics in the CaO-MgO-SiO_2 system with B_2O_3, P_2O_5, Na_2O and CaF_2 additives", J. Eur. Ceram. Soc., 2006, 26, 1463-1471.

[34]. Nemati, A., Goharian, P., Shabanian, M. and Afshar, A., "Effects of nucleation agent particle size on properties, crystallisation and microstructure of glass-ceramics in TiO_2-ZrO_2-Li_2O-CaO-Al_2O_3-SiO_2 system", Adv. Appl. Ceram., 2010, 109, 318-323.

[35]. Clausbruch, S. C., Schweiger, M., Hooland, W. and Rheinberger, V., "The effect of P_2O_5 on the crystallization and microstructure of glass-ceramics in the SiO_2-Li_2O-K_2O-ZnO-P_2O_5 system", J. Non-Cryst. Solids, 2000, 263&264, 388-394.

[36]. Ghosh, S. B., Reaney, I. M., Gillingham, K. H., Brook, I. M. and Hatton, P. V., "Evaluation of modified fluorcanasite glass-ceramics for bone tissue augmentation", Key Eng. Mater., 2005, 284-286, 557-560.

[37]. Ghosh, S. B., Reaney, I. M., Johnson, A., Gillingham, K. H., Brook, I. M. and Hatton, P. V., "The effect of investment materials on the surface of cast fluorcanasite glasses and glass-ceramics", J. Mater. Sci.: Mater. Med., 2008, 19, 839-846.

[38]. Ohlberg, S. M. and Strickler, D. W., "Determination of percent crystallinity of partly devitrified glass by X-ray diffraction", J. Am. Ceram. Soc., 1962, 45, 170-171.

[39]. ASTM C 1161: Standard Test Method for Flexural Strength of Advanced Ceramics at Ambient Temperature.

[40]. ASTM C 1328-08: Standard Test Method for Vickers Indentation Hardness of Advanced Ceramics.

[41]. Chantikul, P., Anstis, G. R., Lawn, B. R. and Marshall, D. B., "A critical evaluation of indentation techniques for measuring fracture toughness: II, Strength method", J. Am. Ceram. Soc., 1981, 64, 539-543.

[42]. Lawn, B. R. and Marshall, D. B., "Hardness, toughness, and brittleness: An indentation analysis", J. Am. Ceram. Soc., 1978, 62, 347-350.

[43]. Clausbruch, S. C., Schweiger, M., Holand, W. and Rheinberger, V., "The effect of P_2O_5 on the crystallization and microstructure of glass-ceramics in the SiO_2-Li_2O-K_2O-ZnO-P_2O_5 system", J. Non-Cryst. Solids, 2000, 263-264, 388-394.

[44]. Attar, S. G., "Fluorcanasite glass-ceramics for dental applications", (Doctoral dissertation), The University of Sheffield, 2005.

[45]. Kanchanarat, Miller, C., Hatton, P. V., N., James, P. F. and Reaney, I. M., "Early stages of crystallization in canasite-based glass-ceramics", J. Am. Ceram. Soc., 2005, 88, 3198-3204.

[46]. Wheaton, B. R. and Clare, A. G., "Evaluation of phase separation in glasses with the use of atomic force microscopy", Journal of Non-Crystalline Solids, 353 (52-53), (2007), 4767-4778.

[47]. Steinbrech, R. W., "Toughening mechanisms for ceramic materials", J. Eur. Ceram. Soc., 1992, 10, 131-142.

[48]. Rozhdestvenskaya, I. V., Nikishova, L. V., Lazeanik, K. A., "The crystal structure of frankamenite", Mineral. Mag., 1996, 60, 897-905.

[49]. Boccaccini, A. R., "Machinability and brittleness of glass-ceramics", J. Mater. Process. Technol., 1997, 65, 302-304.